Supplement of Atmos. Chem. Phys., 16, 3369–3382, 2016
http://www.atmos-chem-phys.net/16/3369/2016/
doi:10.5194/acp-16-3369-2016-supplement

Atmospheric Chemistry and Physics Open Access EGU

Supplement of

Top-down estimates of benzene and toluene emissions in the Pearl River Delta and Hong Kong, China

Xuekun Fang et al.

Correspondence to: Xuekun Fang (fangxk@mit.edu) and Min Shao (mshao@pku.edu.cn)

Table S1. Information about meteorological measurement stations in the domain (111.45°E−118.15°E, 21.70°N−27.33°N) in southern China. This information, as well as the meteorological measurement data, was obtained from http://gis.ncdc.noaa.gov/map/viewer/#app=cdo&cfg=cdo&theme=hourly&layers=1&node=gis.

ID	Station name	Country or region	Latitude	Longitude	Elevation (m)
450070	HONG KONG INTL	HONG KONG	22.31	113.92	8.5
450110	MACAU INTL	MACAU	22.15	113.59	6.1
450320	TA KWU LING	CHINA	22.53	114.15	13.0
450350	LAU FAU SHAN	CHINA	22.47	113.98	35.0
450390	SHA TIN	CHINA	22.40	114.20	8.0
450440	CHEUNG CHAU	CHINA	22.20	114.02	79.0
577660	SHAOYANG	CHINA	27.18	111.45	310.4
577760	NANYUE	CHINA	27.30	112.70	1268.0
577990	JI'AN	CHINA	27.12	114.97	78.0
578660	LINGLING	CHINA	26.23	111.62	174.0
579720	CHENZHOU	CHINA	25.73	112.97	368.8
579930	GANZHOU	CHINA	25.85	114.95	125.0
587250	SHAOWU	CHINA	27.33	117.47	219.0
588130	GUANGCHANG	CHINA	26.85	116.33	142.0
588340	NANPING	CHINA	26.63	118.15	153.0
589110	CHANGTING	CHINA	25.85	116.37	311.0
589210	YONG'AN	CHINA	25.97	117.35	204.0
589260	ZHANG PING	CHINA	25.30	117.40	203.0
589310	JIUXIAN SHAN	CHINA	25.72	118.10	1651.0
590720	LIANZHOU	CHINA	24.80	112.37	98.0
590820	SHAOGUAN	CHINA	24.67	113.60	68.0
590870	FOGANG	CHINA	23.88	113.52	68.0
590960	LIANPING	CHINA	24.37	114.48	214.0
591020	XUNWU	CHINA	24.95	115.65	299.0
591170	MEI XIAN	CHINA	24.28	116.07	116.9
591340	GAOQI	CHINA	24.54	118.13	18.0
592780	GAOYAO	CHINA	23.05	112.47	12.0
592870	BAIYUN INTL	CHINA	23.39	113.30	15.2
592930	HEYUAN	CHINA	23.80	114.73	41.0
593160	SHANTOU	CHINA	23.40	116.68	3.0
594930	BAOAN INTL	CHINA	22.64	113.81	4.0
595010	SHANWEI	CHINA	22.78	115.37	5.0
596630	YANGJIANG	CHINA	21.87	111.97	22.0
596730	SHANGCHUAN DAO	CHINA	21.73	112.77	18.0

Table S2. Performance comparison of simulating benzene and toluene mixing ratios at the Heshan site using the gridded emissions estimated by RCP 2.6, Yin et al. 2015, REAS v1.1 REF, MEIC v1.2 and this study. $\boldsymbol{E}$ is the root mean square error (RMSE) for the bias between the simulated and observed mixing ratios. $\boldsymbol{B}$ denotes the mean bias between the simulated and observed mixing ratios. $\boldsymbol{r^2}$ represents the squared Pearson correlation coefficients between the simulated and observed mixing ratios.

	Benzene simulation			Toluene simulation		
	E	B	r^2	E	B	r^2
RCP 2.6	1.396	0.783	0.195	5.80	4.65	0.054
Yin et al. 2015	1.489	0.645	0.244	5.30	4.02	0.069
REAS v1.1	2.237	1.871	0.083	5.67	4.44	0.023
MEIC v1.2	1.491	0.941	0.198	5.00	1.56	0.042
This study	1.262	0.409	0.268	4.30	1.99	0.097
This study performed best?	Yes	Yes	Yes	Yes	No	Yes

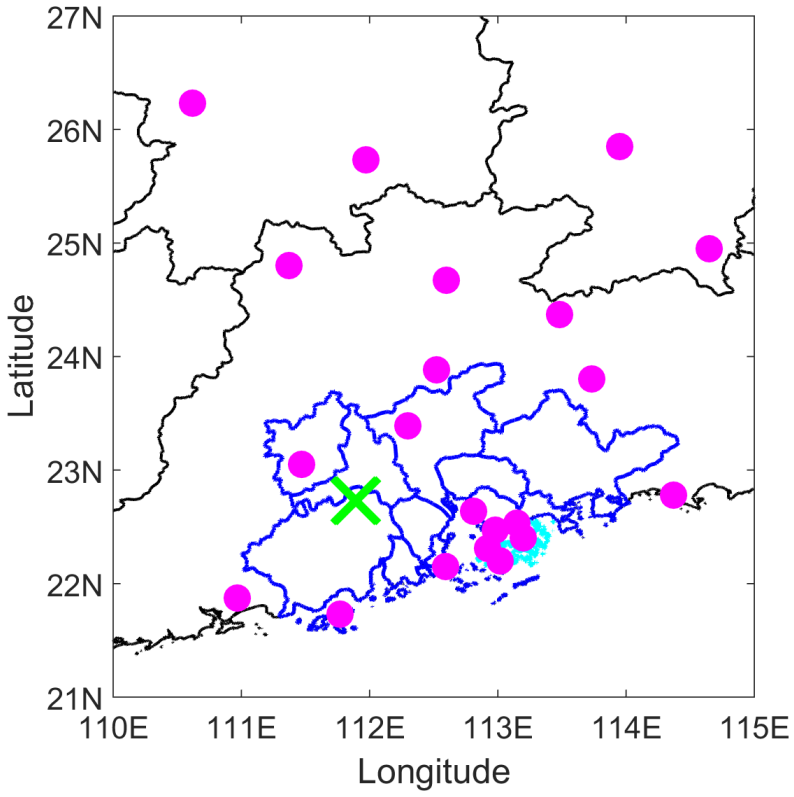

Figure S1**.** Map of meteorological measurement stations. The green cross indicates the location of the Heshan observation site (measuring benzene and toluene). The solid pink circles indicate the locations of the meteorological measurement stations. The PRD region is indicated by dark blue boundary lines and the Hong Kong region with cyan boundary lines.

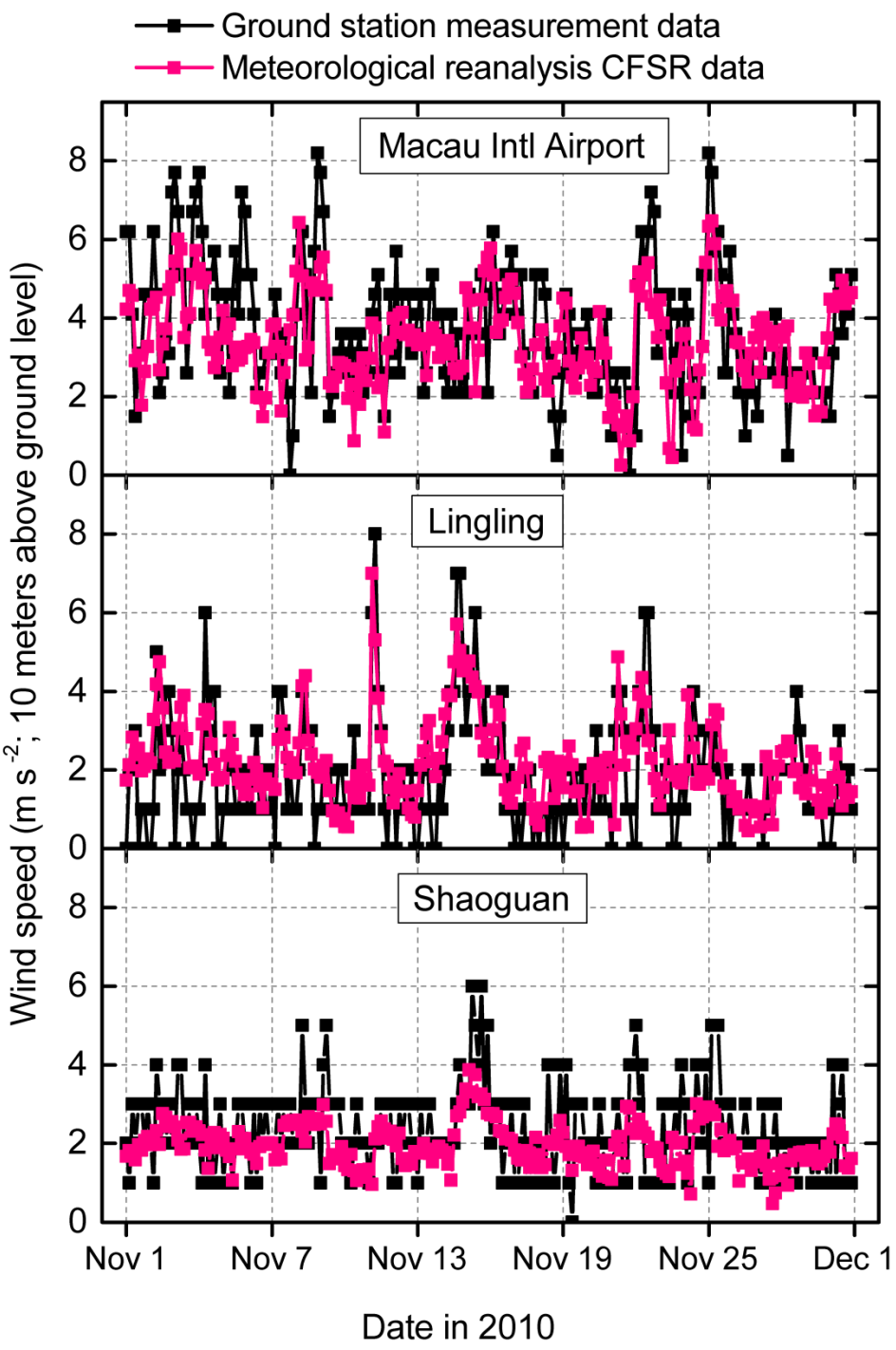

36

37 Figure S2. Wind speed at 10 meters above ground level from meteorological reanalysis CFSR data and
38 observed at three stations (Macau Intl Airport, Lingling and Shaoguan).

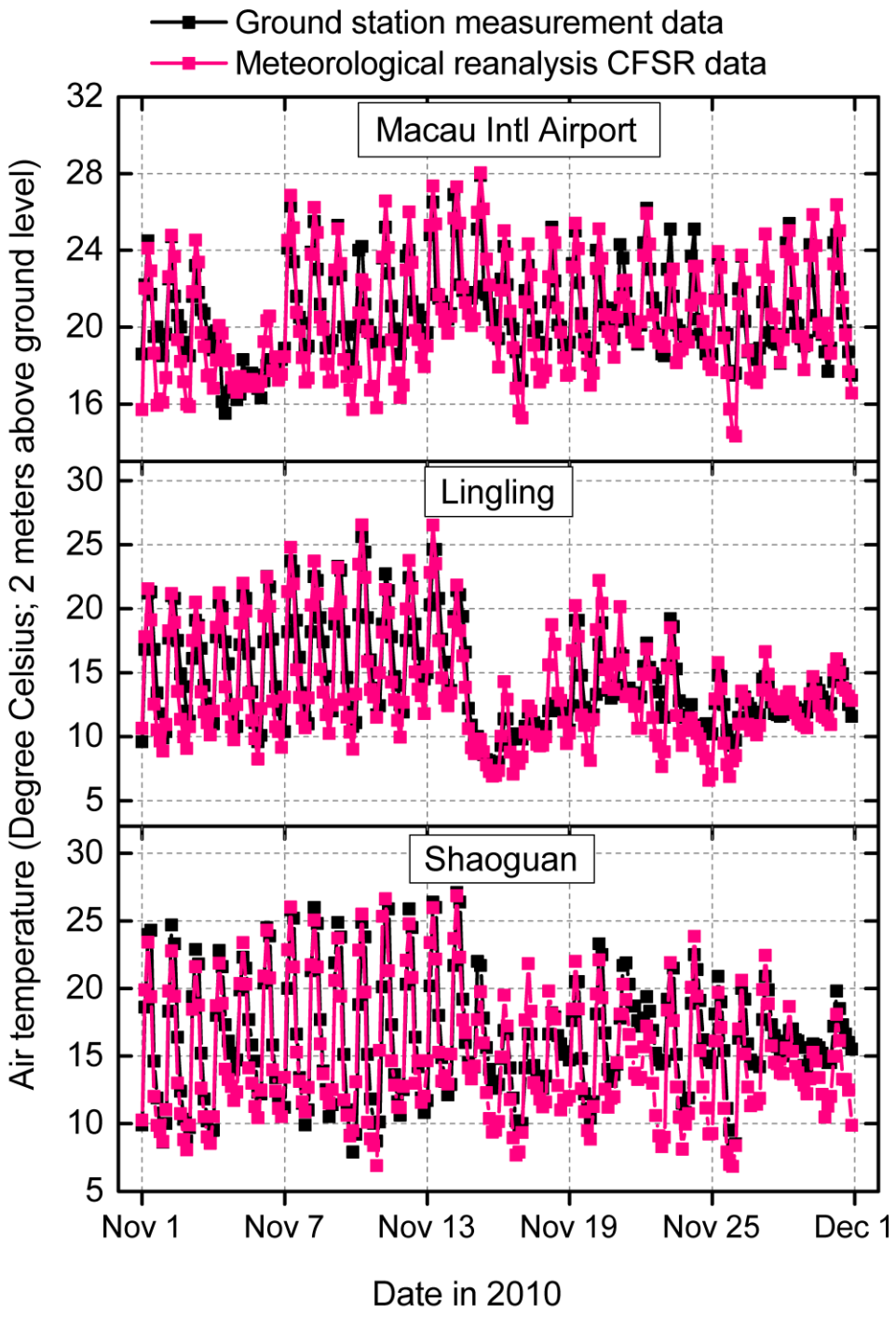

39

40 Figure S3**.** Air temperature at 2 meters above ground level from meteorological reanalysis CFSR data and
41 observed at three stations (Macau Intl Airport, Lingling and Shaoguan).

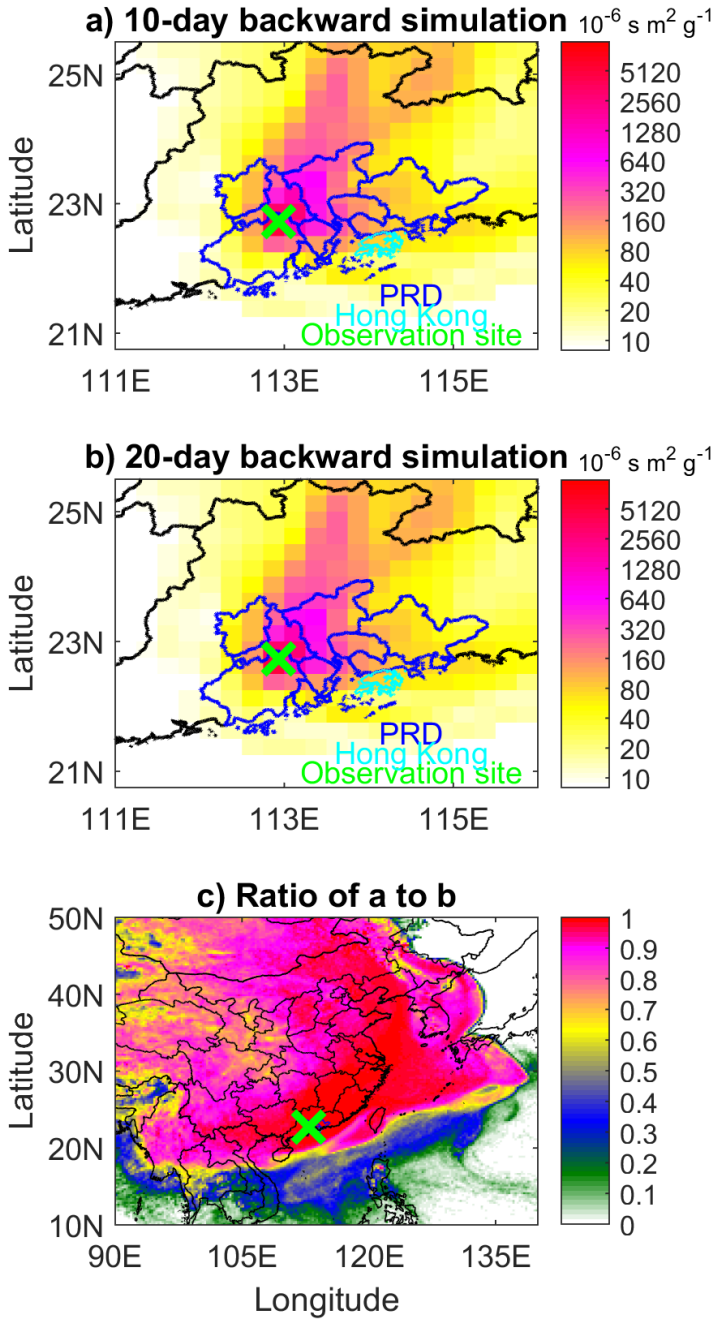

42

43 Figure S4. Spatial distribution of the average benzene emission sensitivities a) from a 10-day backward
44 simulation, b) from a 20-day backward simulation, and c) the ratio of a to b for the observation period.
45 Note that the domain size in c) is not the same as in a) and b).

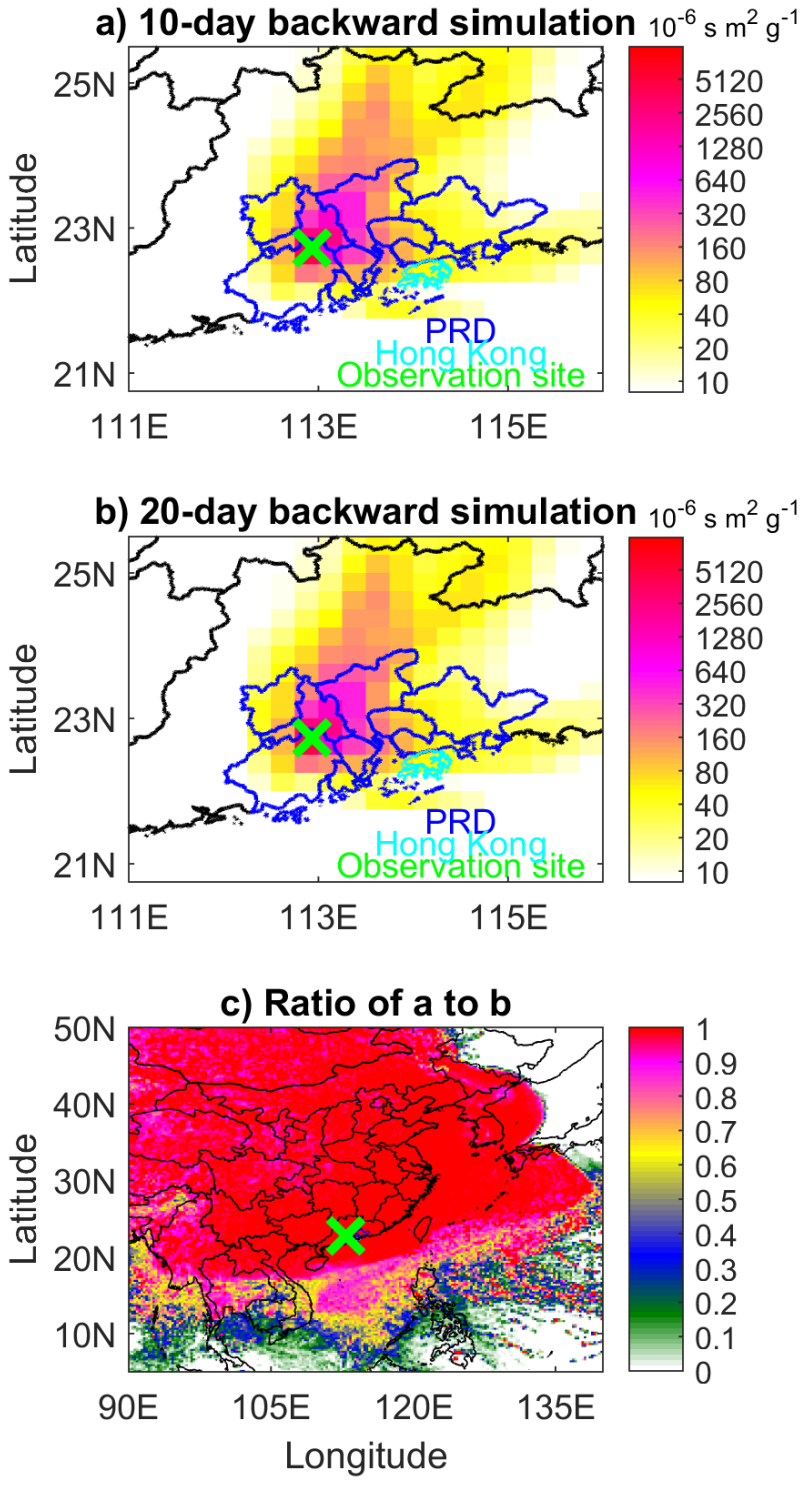

46

47 Figure S5. Spatial distribution of the average toluene emission sensitivities a) from a 10-day backward
48 simulation, b) from a 20-day backward simulation, and c) the ratio of a to b for the observation period.
49 Note that the domain size in c) is not the same as in a) and b).

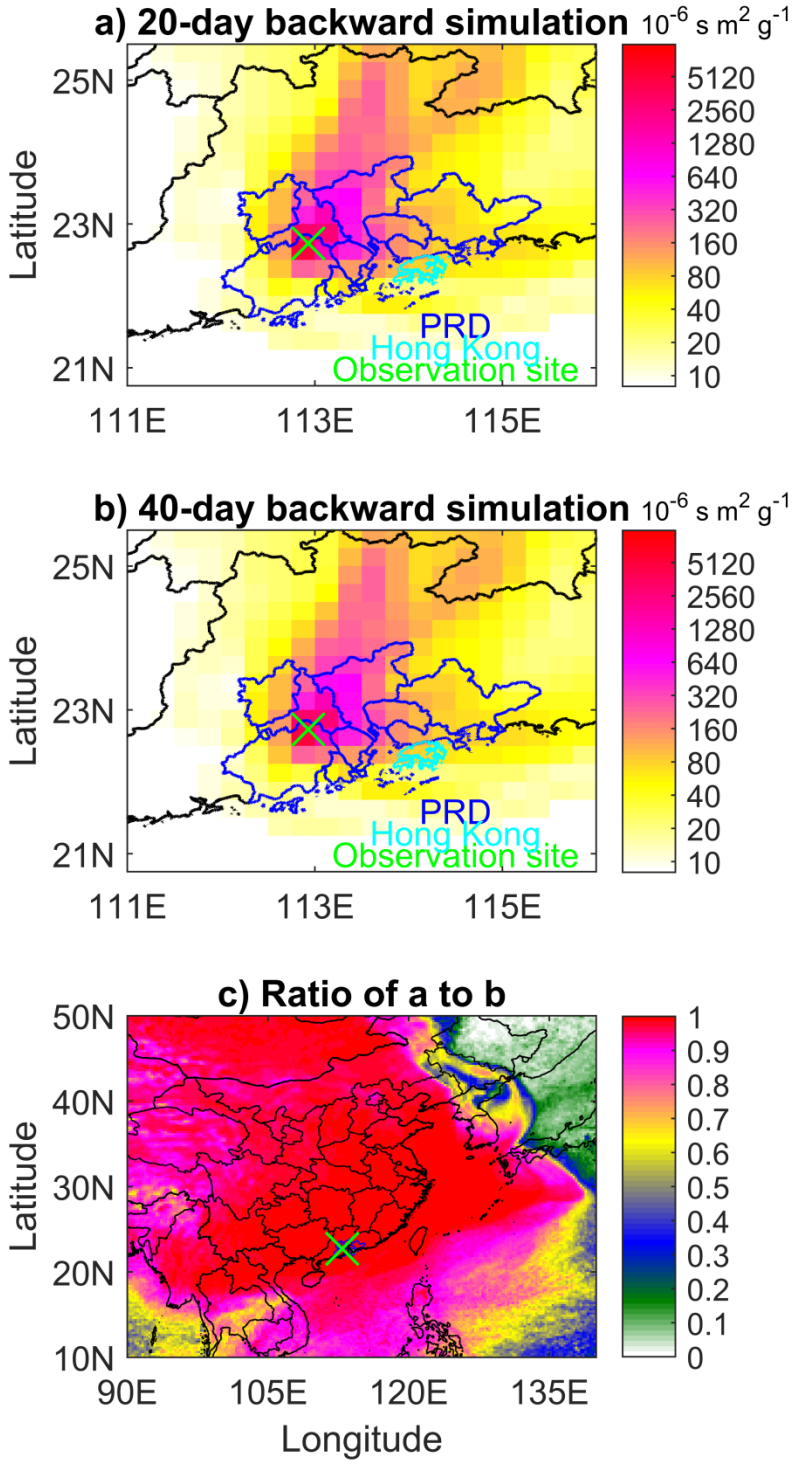

Figure S6. Spatial distribution of the average benzene emission sensitivities a) from a 20-day backward simulation, b) from a 40-day backward simulation, and c) the ratio of a to b for the observation period. Note that the domain size in c) is not the same as in a) and b).

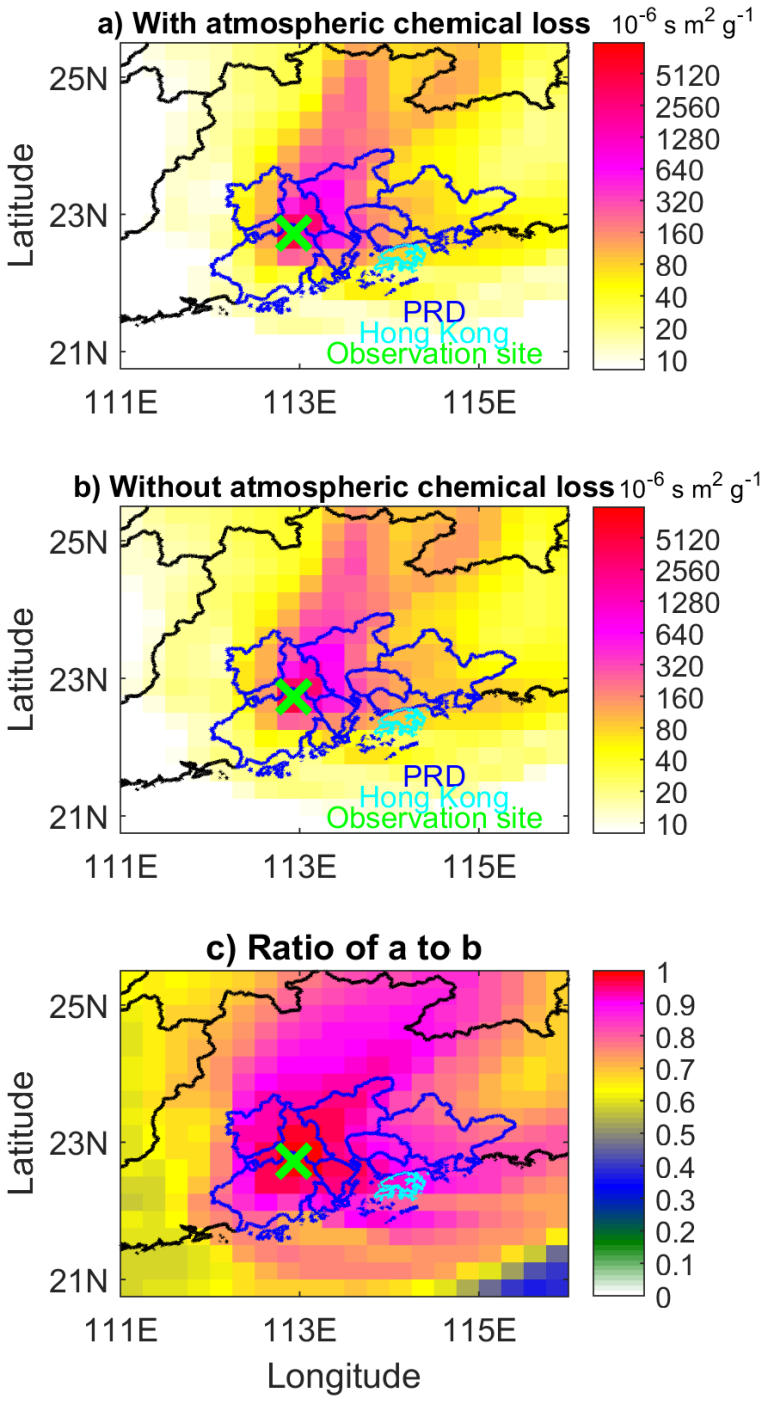

54

55 Figure S7. Spatial distribution of the average toluene emission sensitivities a) with atmospheric chemical
56 loss, b) without atmospheric chemical loss, and c) the ratio of a to b for the observation period.

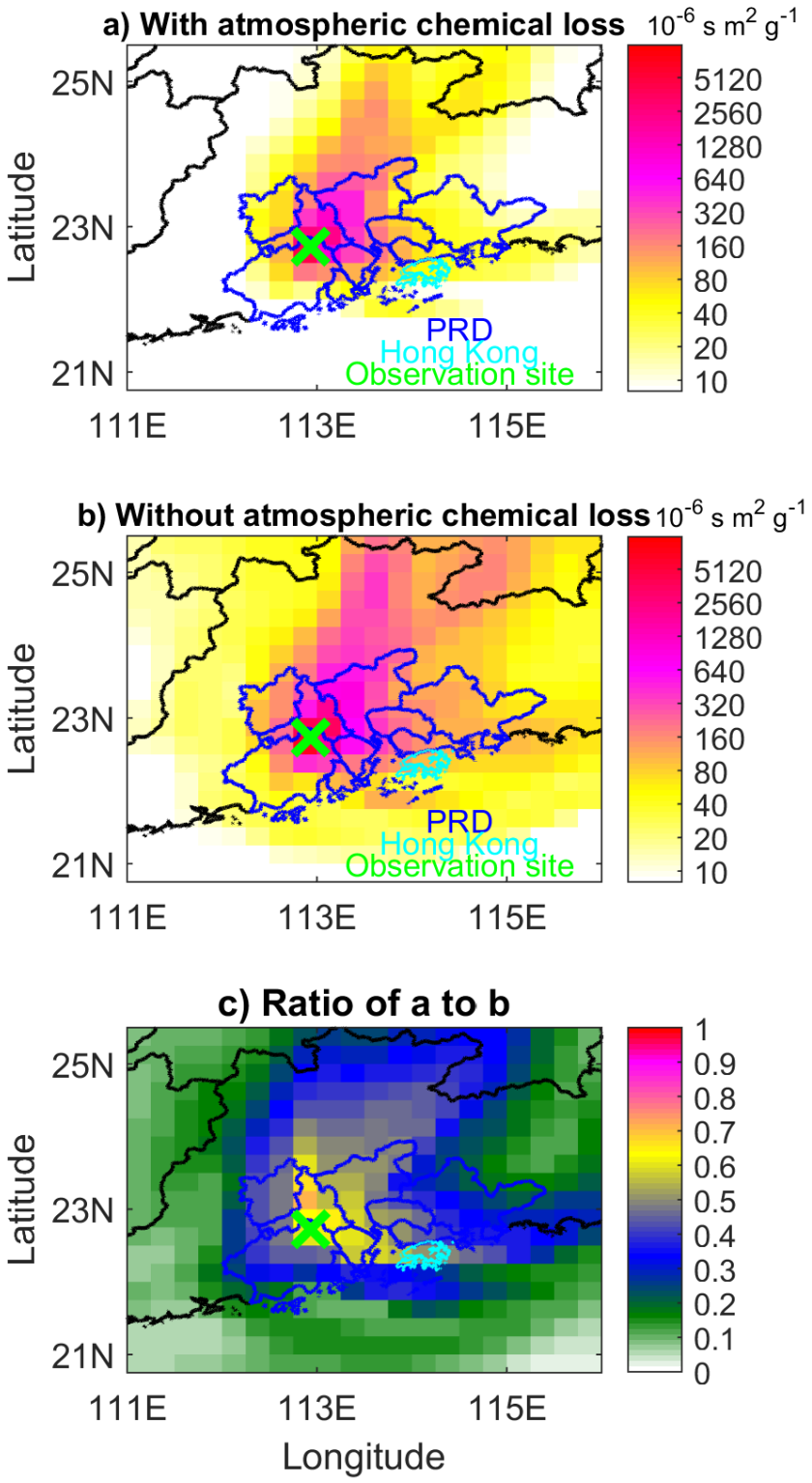

57

58 Figure S8. Spatial distribution of the average toluene emission sensitivities a) with atmospheric chemical
59 loss, b) without atmospheric chemical loss, and c) the ratio of a to b for the observation period.

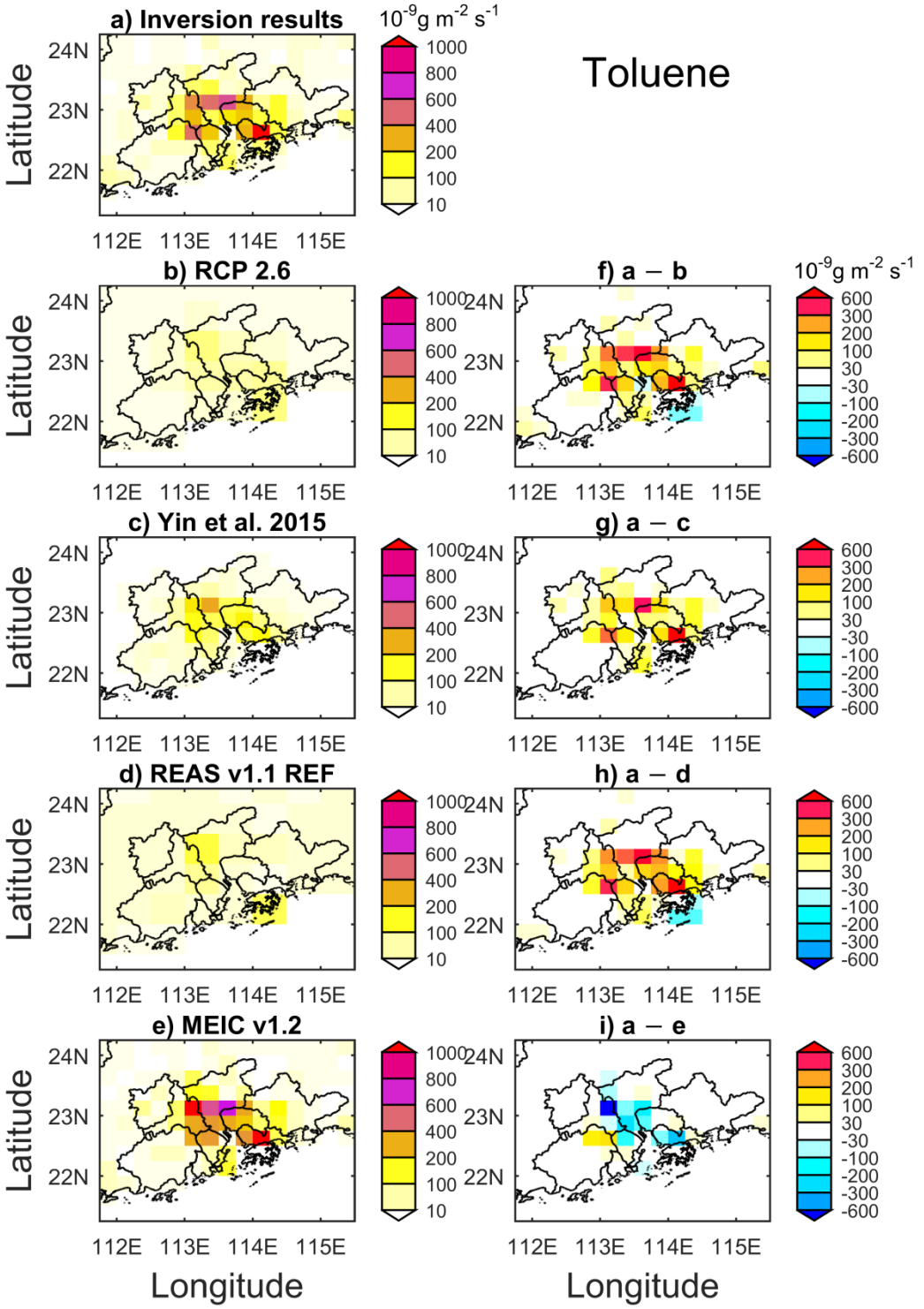

Figure S9. Maps of toluene emissions for PRD, HK and surrounding regions from a) inversion, b) RCP 2.6, c) Yin et al. (2015), d) REAS v1.1 REF, e) MEIC v1.2, and the difference between inversion results (a) and the bottom-up inventories (b, c, d, e). Note that in c) and g) only emissions within PRD are plotted since Yin et al. (2015) only estimated emissions within PRD, and that in e) and i) emissions within HK are not plotted since MEIC v1.2 has not estimated toluene emission in HK.

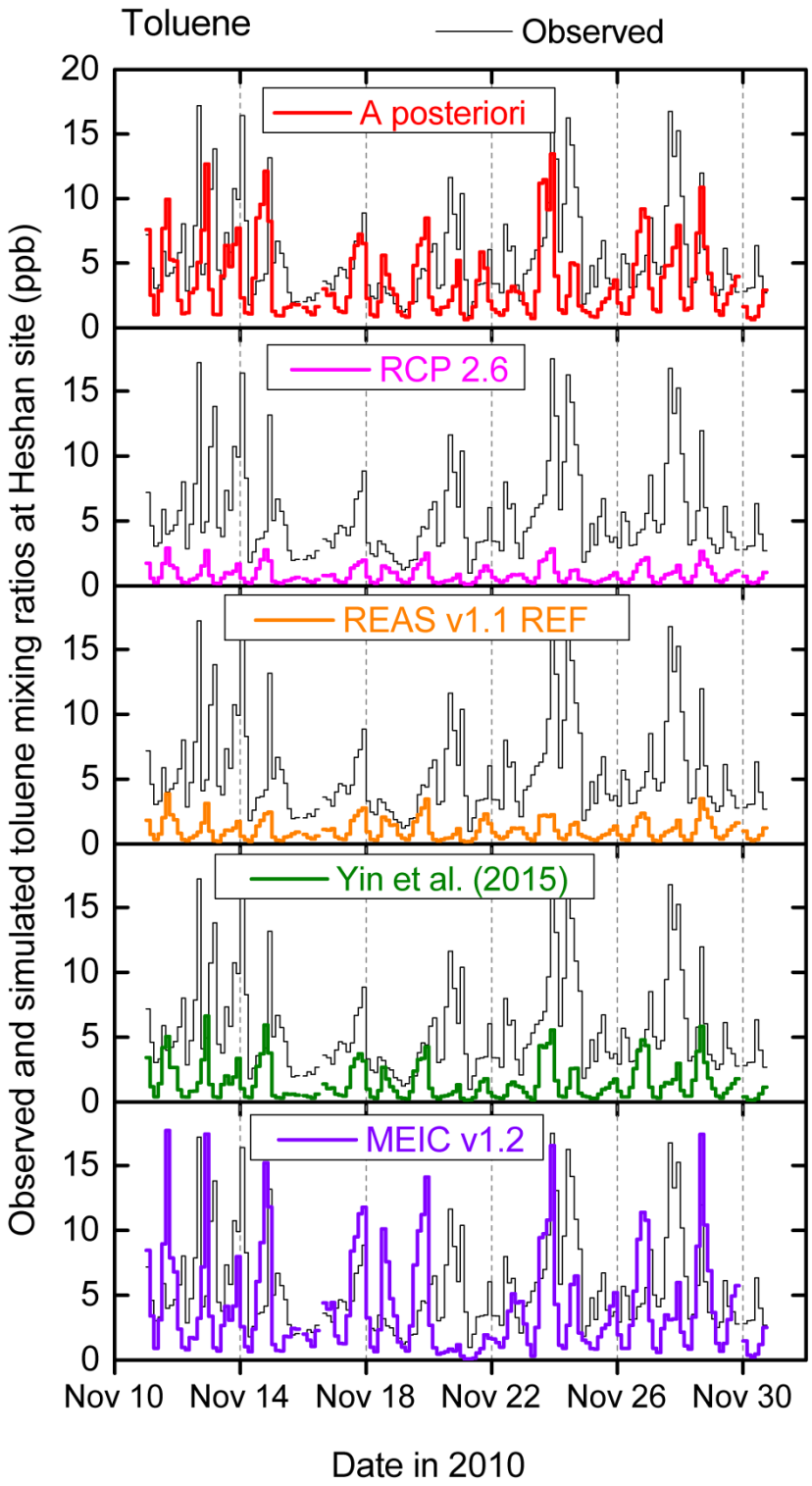

Figure S10. Time series of observed and simulated toluene mixing ratios at the Heshan site. The simulations use emission fields from inversion in this study, RCP 2.6, REAS v1.1 REF, Yin et al. (2015) and MEIC v1.2, respectively.